Investigation of charge transport in single OPE3 molecules

THESIS

submitted in partial fulfillment of the
requirements for the degree of

MASTER OF SCIENCE
in
PHYSICS

Author :	Jurriën van der Loo
Student ID :	s1378325
Supervisor :	Prof. Jan M. van Ruitenbeek
	Sasha Vrbica
2^{nd} corrector :	Asst. Prof. Milan Allan

Leiden, The Netherlands, June 14, 2018

Investigation of charge transport in single OPE3 molecules

Jurriën van der Loo

Huygens-Kamerlingh Onnes Laboratory, Leiden University
P.O. Box 9500, 2300 RA Leiden, The Netherlands

June 14, 2018

Abstract

Using the notched wire mechanically controllable break junction technique charge transport of a single-molecule junction, containing the OPE3 molecule, is studied at room temperature. By deposition of molecules from solution between two gold leads we were able to determine the conductance of the OPE3 at $(1.6 \pm 0.3) \cdot 10^{-4} G_0$. The measurement speed of the LabVIEW control program for this experiment was improved by more than a factor of 7 compared to the previous version.

Chapter 1

Introduction

Ever since the invention of the transistor in 1947 by Bardeen, Brattain and Shockley [1] the electronics industry has evolved into the unmissable presence it is nowadays. In the ongoing quest of reducing the size of electronic components to a minimum, microelectronics has become a very important branch of this industry. Downscaling transistors, diodes, resistors, capacitors and the likes over about 70 years has resulted in circuit parts that are just several tens of nanometers in size. Currently, a miniscule 10 nm transistor is already used in a microprocessor [2].

Fabrication of electronic components below the size of 10 nm comes with its own set of rules. The production methods of today have not yet proven that they can deliver such material without losing on performance [3]. So, as engineers are approaching the limit to the minimization of electronic circuits, other methods and designs have to be considered in order to keep reducing the size of integrated circuits, or chips, all while keeping them as efficient as before or even improving them in the process. Further size reduction would mean that the components are to consist of only a few atoms. In order to achieve this an auspicious approach is pursued [4], that was proposed as early as the 1960s, to use specific single molecules and their properties in a circuit. In 2000 a first working molecular switch was created [5] paving the way for further research and development.

Before the first *molecular electronic circuit* can be developed it is necessary to gain knowledge about the electronic properties of metallic electrodes that contact single molecules. By and large, this is what the field of molecular electronics deals with. There are various methods to investigate metallic contacts and make accurate measurements. In recent years

the most common methods [6] were based on the use of the scanning tunnelling microscope (STM), the atomic force microscope (AFM) and the electromigration technique, among others. One other method, that was also used in this research, is the mechanically controllable break junction (MCBJ) technique.

In a 1985 article by Moreland et al. [7] a new method to measure a tunneling current is described. By breaking a junction between two metallic electrodes a small gap originates, in which a tunneling current can flow. Through gentle bending of a flexible glass beam it is possible to control the tunneling resistance. This idea is the inception of the MCBJ technique as it came to be called a few years later. Muller et al. [8] described it in the title of their article as 'the transition from weak link [of atoms] to tunnel junction'. The most notable advantage was the ability to control the transition between the 'weak link' and 'tunnel junction', effectively being able to break and reform the junction on the atomic level. Another advantage of this technique is that breaking of the wire results in sharp electrode tips, which means that charge transport takes place mainly through one or a few atoms [9].

Five years after this breakthrough, Reed et al. [10] were first to use the MCBJ technique to measure charge transport in organic molecules. There are several ways to create an atomic contact for MCBJ, using lithography for instance. Here, a pattern of two metal leads can be fabricated on a wafer substrate as a relief structure by removing parts of the layer on top of the substrate with an electron beam so that only the leads remain [11]. The result is a structure with an atomic contact between the small electrodes. However, it is hard to deposit a solution with molecules between the electrodes, which is an important aspect of this research. Also, the slow breaking of lithographic samples compared to other methods, while allowing for very precise control of electrode separation, increases the lifetime of a molecular junction, which affects the accuracy of conductance measurements [12].

In this research the notched wire break junction is used, where a circular notch is created on a solid wire. The preparation time for this method is considerably shorter than for lithographic methods. Additionally, the measurement speed is higher, so it is possible to collect more data and subsequently perform a better statistical analysis. One drawback is that the atomic contact around the notch is different for every sample and that it is cumbersome to create a notch that is still in contact yet almost broken.

The lithographic break junction produces atomic contacts more reliably and more consistently in that respect.

Chapter 2

Theory

Measuring the electrical conductivity of atoms or molecules is the main objective of this experiment. Whilst a conductivity measurement is essentially similar for any material of any size, it becomes harder to perform for smaller scaled systems. Generally, at the *macroscopic* level electrical elements at the size of circuitry are considered. In most of these cases one can safely rely on Ohm's law to calculate the conductance. On a smaller scale, the *mesoscopic* or even microscopic level, where quantum effects start to take place, this relation does not hold anymore and a different approach is required. After a brief recap of conductance with Ohm's law a more extensive treatment is given to the physics of electrical conductance at the mesoscopic scale. This eventually leads to the definition of the quantum of conductance, a value for the conductance of a metal with a single-atom contact. In the final section the principles of electrical transport in molecules are covered.

2.1 Conductance

Conductance is a measure of how easily electric charge flows in a material. The flow is accomodated by charge carriers, with electrons and holes [13] being the carriers in metals. One way to think of the conductance, or resistance for that matter, is in line with the Drude model of conductivity. It states that electrons collide with other particles in the conducting material. Electrons experience resistance as they flow through the conductor, losing momentum in the process. This is quantified as the conductivity σ; an empirically determined constant, which is unique for each material.

Ohm's law can be used in most instances of metallic materials. The general form of Ohm's law is $J = \sigma E$, where J is the current density and E is the electric field. A more familiar form of Ohm's law is $I = UR$, where the current I is directly proportional to the voltage U by a factor R. The conductance G is the reciprocal of R. In the macroscopic regime this formula works very well. Once the length of the conductor becomes very small, however, the conductance should increase to extremely large values. Or, in other words, with a very small wire length a resistance that approaches zero is expected. One can even think of a situation in which the electron is not involved in any collision while moving through the short wire, the so-called ballistic regime. If this is the case, it could be argued that the resistance is zero. Experiments have shown that there is no zero resistance in atomic-sized contacts [14], so how does this resistance come about?

2.2 Landauer formula

A popular way to describe conductance on the mesoscopic scale is via the Landauer approach. It considers a simple system of two metallic leads coupled with a piece of conductor. The current through the conductor will be taken as the probability for an electron to travel from one lead to the other through the conductor. This probability depends on whether the electron wave function is transmitted or reflected at the boundary of the leads and the conductor, which is why this is also referred to as the scattering approach.

Closely following the derivation of the Landauer formula for the current in the scattering approach as performed by *Cuevas and Scheer* [6], first a number of assumptions has to be made. The two metallic leads act as ideal electron reservoirs, described by a Fermi-Dirac distribution for the electrons, $f(E) = 1/(1 + e^{(E-\mu)/kT})$. Here k is Boltzmann's constant, T is the temperature, E is the particle energy and μ is the chemical potential of the leads, also referred to as the Fermi energy. The reservoirs are in thermal equilibrium, each with a well-defined temperature and Fermi energy. Also, all collisions in the wire involving electrons are taken to be elastic. Only in the reservoirs inelastic scattering occurs, but this does not affect the charge transport. Finally, the derivation starts from the viewpoint of a single electron and the current it carries.

Following the basic principles of quantum mechanics the moving elec-

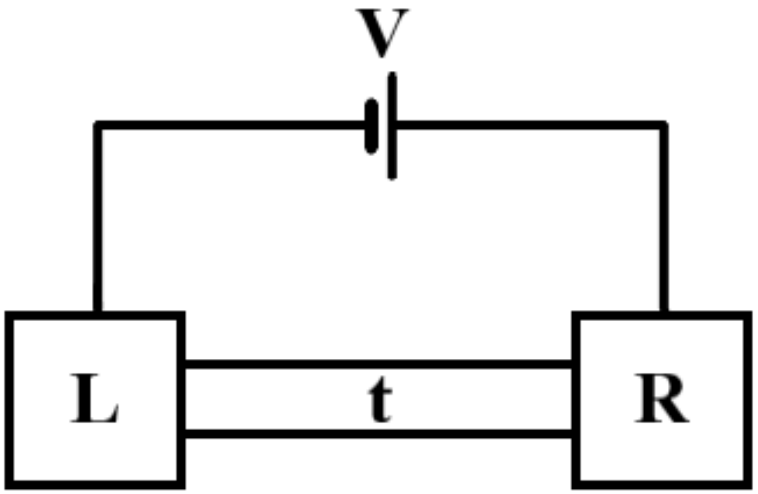

Figure 2.1: *Simplified schematic of two metallic leads connected with a conducting wire. The left lead, with Fermi energy $E_{F,l}$, is labeled L and the right lead, with Fermi energy $E_{F,r}$, is labeled R. The probability that an electron traverses the wire is given by the square of the transmission coefficient $|t|^2$. Applying a bias voltage V will result in a shift of the Fermi energies of the leads.*

tron has a wave function. This is given in the form of a plane wave, which is normalized to the length L of the wire: $(1/\sqrt{L})e^{ikx}$. Each electron wave function has a transmission coefficient t, which gives the amplitude of the wave. The probability that the electron traverses the wire is then given by $|t|^2$. Electrons fill the discrete energy levels of the metal lead up to the Fermi energy. A current can only flow when an occupied level in the left reservoir is empty in the right reservoir, leading to the following expression for all participating electrons (see Figure 2.1):

$$I_{L\to R} = \frac{e\hbar}{2\pi}\int dk \frac{k}{m} T(k) f_L(k)[1 - f_R(k)],$$

where m is the electron mass and $T(k) = |t|^2$ is the transmission function.

In order to simplify the rest of the derivation, it is assumed that the conductance electrons in the wire are described by an ideal one-dimensional Fermi gas. This implies the following expression for the energy: $E = \hbar^2 k^2/(2m)$.

Using this expression the current from left to right can be written as

$$I_{L\to R} = \frac{e}{h}\int dE T(E) f_L(E)[1 - f_R(E)].$$

A similar expression can be derived for the current from the right to the left lead, $I_{R\to L}$, with every L substituted for an R and vice versa.

The net current flow is obtained by subtracting $I_{R\to L}$ from $I_{L\to R}$:

$$I(U) = \frac{2e}{h}\int dET(E)[f_L(E) - f_R(E)],$$

where the extra factor of 2 is due to the spin degeneracy of the electrons. This completes the derivation of the Landauer formula in its simplest form and by taking some liberties with assumptions and approximations. Still, it is very instructive as a relation between the current and the transmission of the conductor and has proven to be rather precise.

2.3 Quantum of conductance

While the term $\frac{2e}{h}$ in the Landauer formula is a constant, the transmission function and the Fermi-Dirac functions are dependent on the energy and are therefore variable. It is feasible, however, to fix the Fermi-Dirac functions by assuming $T = 0$ K in the system, which results in all energy levels until the Fermi energy being fully occupied on both leads. This way it becomes the step function $\Theta(\mu_0 - E)$, with μ_0 the Fermi energy at $T = 0$ K [15]. By applying a bias voltage V to the system the Fermi energy can be manipulated, resulting in an increased μ_0 on the left lead and an equally decreased value on the right lead or vice versa.

As long as the bias voltage is kept low the difference between the Fermi energies of the left and right lead also remains small and it can safely be assumed that the transmission function is independent of the energy. The integral of the Landauer formula can be solved for the step functions of both leads and can be rewritten as:

$$I(U) = \frac{2e}{h}T(\mu_0 + \frac{eV}{2} - (\mu_0 - \frac{eV}{2})) = \frac{2e^2}{h}TV.$$

This means that for a wire with a perfect single conductance channel ($T = 1$) there will always be a finite conductance of $G_0 = \frac{2e^2}{h}$, which is called the *quantum of conductance*.

Version of June 14, 2018– Created June 14, 2018 - 11:25

2.4 Transport in metal-molecule-metal junctions

So far only the current from one metal lead directly to another has been considered. It was implied that the two leads have a Fermi energy and that a bias voltage can be used to increase or decrease the chemical potential of a lead. When a molecule is placed in the junction the transport between the two leads has a different character.

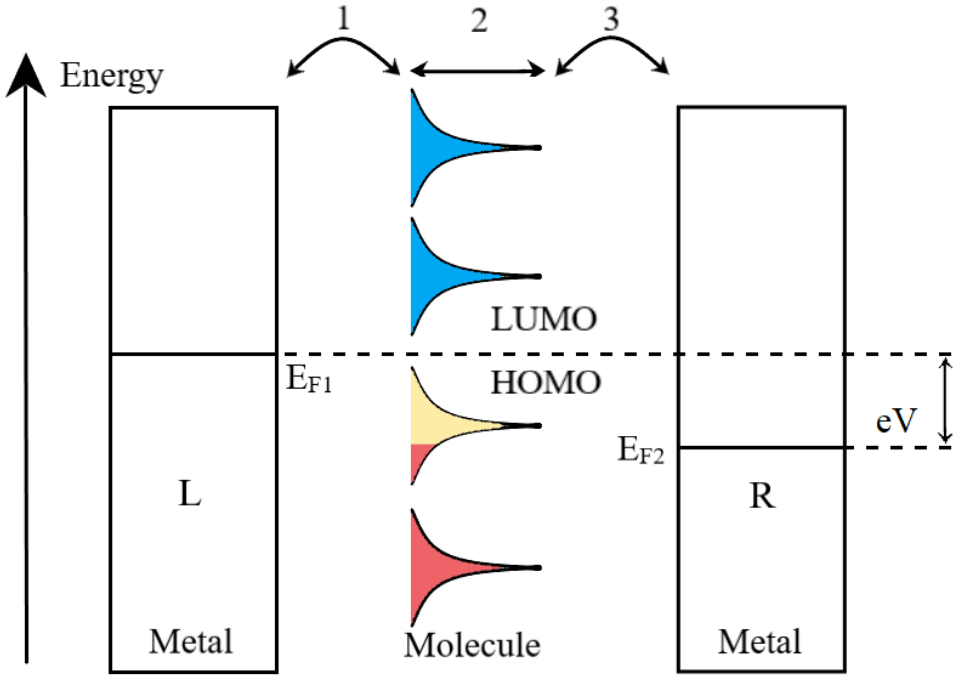

Figure 2.2: *Schematic depiction of a metal-molecule-metal junction with an applied bias voltage (V). Part 1 shows the transport from the left metal lead L to the molecule, whereas part 3 shows the transition from the molecule to the right metal lead R. Part 2 concerns the filling of the molecule's electron levels. Red regions denote occupied parts of the electron level, blue regions are unoccupied. The light yellow region is partially occupied due to simultaneous filling from the left lead and emptying from the right lead.*

Molecular transport in a junction can be divided into three main parts (see Figure 2.2) [16]. First there is the electrode-molecule interface, which is where the molecule is coupled to the metal electrode. There are multiple stages in the coupling, which will be discussed shortly. Following the Landauer principle, the electron has a probability of travelling from the

electrode to the molecule. Then, the molecule has multiple discrete energy levels that can be occupied, called *molecular orbitals*. Two electrons fill up one orbital and the orbitals are filled from lowest to highest energy. With all the electrons occupying various orbitals, one occupied orbital has the highest energy and one unoccupied orbital has the lowest energy. These are the *highest occupied molecular orbital* (HOMO) and the *lowest unoccupied molecular orbital* (LUMO), respectively. HOMO and LUMO in particular play an important role in charge transport. Finally, in part 3, the electron has a probability of travelling from the molecule to the other electrode.

The orbitals in Figure 2.2 that have a red shaded area are fully occupied, whereas the blue shaded areas refer to orbitals that are completely unoccupied. The HOMO level is filled by the left lead, but simultaneously emptied by the right lead, hence it experiences a partial occupation and its area is shaded a light yellow. The shape and the energy of the orbitals is modified by the interaction of the metal leads with the molecule [17]. With the molecule unbound to any of the leads, the orbitals are at discrete energies. Once the molecule is approaching the metal leads long-range physical interactions between atoms and molecules, such as van der Waals forces, start to play a role. The effects of these kind of distant interactions are referred to as *physisorption* [18] (see Figure 2.3). There is not yet any notable charge transport, but as the molecule comes closer to the metal surfaces the interaction increases. Electron screening effects start to occur in the metal and image charges form on the electrodes. As a consequence the gap between the HOMO and LUMO will continuously decrease.

With the molecule attached to the electrodes the effects of *chemisorption* take place. Due to the chemical bonding between the molecule and the metal surface many of the filled energy levels of the metal lead interact with each individual molecular orbital. The orbitals center around an average value, but interact with many of the levels above and below this value, resulting in a broadening of the molecular energy level. A consequence of broadening of molecular energy levels is that the electrons in the leads have an increased opportunity to occupy the molecular orbitals. The occupation occurs for a short amount of time compared to sharper orbitals, because the interaction with the leads is stronger.

In the meantime, chemical bonding also aligns either the HOMO or the LUMO with the metal's Fermi energy, which establishes a shift of all molecular orbitals to higher or lower energies, respectively. This alignment is also visualised on the right of Figure 2.3, where the HOMO aligns

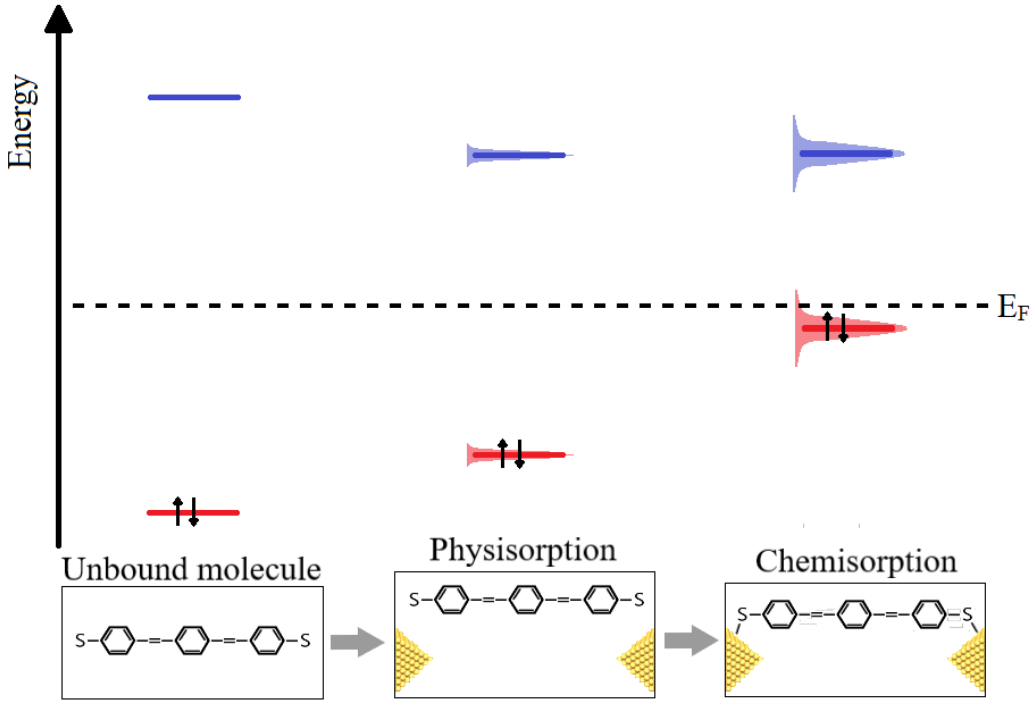

Figure 2.3: *Schematic illustration of the effects of physisorption and chemisorption on the shape of the molecular orbital and the energy level. As the molecule approaches the metal leads the HOMO-LUMO gap starts to decrease, while the molecular orbital density of states is broadened.*

with the Fermi energy. This is the result of a dipole charge forming with the atomic bonding of the metal and the molecule and can also occur due to a small flow of charge, both of which lead to a rigid shift of the molecular orbitals either up or down.

Chapter 3

Mechanically controllable break junction

The conductance experiment is performed using the so-called *dipstick*. With the mechanically controllable break junction (MCBJ) technique it is possible to break the gold wire and reform it again while measuring the current through the wire. Cleaner and more stable break junctions can be obtained in vacuum. For the purpose of this experiment oligo(phenylene ethynylene) (OPE3) molecules contacted with mechanically controllable break junction gold electrodes are investigated.

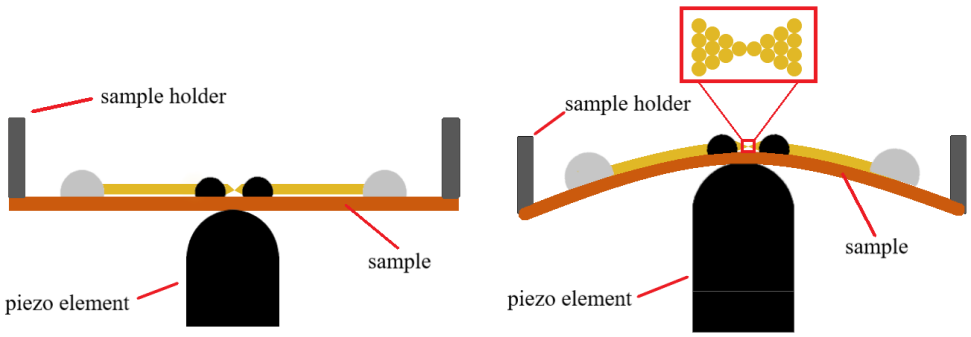

Figure 3.1: *A schematic depiction of a mechanically controllable break junction. The sample consists of a substrate with the gold wire on top. In the middle of the wire is the notch where the breaking occurs. By applying a voltage on the piezo element the sample is pushed in the center, causing a displacement of the gold wire's ends. Before the wire breaks an atomic contact can be established.*

Using the MCBJ technique a notched gold wire is broken by applying

a voltage to a piezo element that pushes on the bottom of the gold wire sample. As the piezo element elongates it slightly displaces the ends of the wire, which breaks the wire around the notch in the middle. By reducing the piezo voltage the junction is mended. In a stable junction it is possible to obtain single-atom conductivity, as shown in Figure 3.1.

3.1 Experimental set-up

We use a home-built dipstick as a measuring instrument. The bottom part contains the sample holder, while the middle part is a hollow cilinder through which the electrical wiring is routed and the top part is equipped with BNC input and output ports.

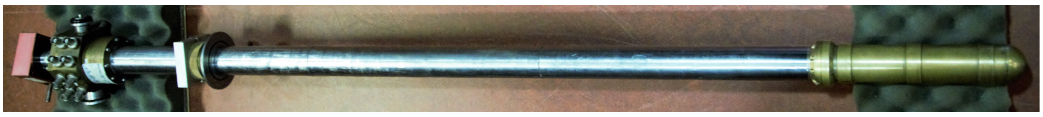

Figure 3.2: *The dipstick, horizontally positioned. At the bottom (right) the sample is placed in the sample holder and at the top (left) all electrical wiring is connected to external ports.*

With the sample placed in the sample holder and connected to the dipstick's internal wiring, BNC cables connect the gold wire to the National Instruments BNC-2110 connector block, which is then connected to the computer equipped with a Data Acquisition (DAQ) card. The line for the current goes from the dipstick to a logarithmic amplifier which has a range of 10^{-10} to 10^{-2} A and a reference current of 10^{-10} A. Current is converted into a voltage in such a way that every power of 10 that exceeds the reference current adds 0.5 V to the output voltage of the amplifier. This is then connected to the input of the connector block. The outputs are the bias voltage V_B and the piezo voltage V_P. Bias voltage is directly relayed to the dipstick and ranges from 40 to 100 mV. Low piezo voltage output of the DAQ ($\pm$ 10 V) is amplified by a voltage amplifier, added to an offset voltage up to a maximum voltage of 750 V and then applied to the piezo element.

For a measurement in vacuum the dipstick is closed by mounting a metal cover on the bottom part of the stick (see Figure 3.2), using an indium wire as a seal. The dipstick is then evacuated with a turbo pump to a pressure of $1 \cdot 10^{-4}$ mbar. For pressures between 0.1 and 500 mbar the

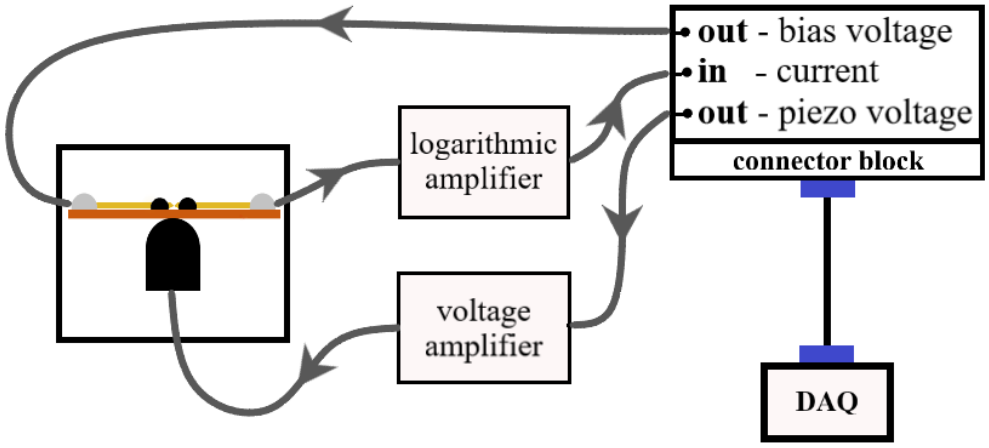

Figure 3.3: *Schematics of the experimental set-up. The DAQ card is implemented in a computer. Bias voltage is applied to the junction, returning a current that is amplified by the logarithmic amplifier and converted to a voltage, which is relayed to the connector block. Piezo voltage is amplified by the voltage amplifier before it is relayed to the piezo element.*

piezo element can start to spark in air [19], which will damage it. Therefore, the piezo voltage is only connected either under ambient conditions or at the base vacuum pressure.

3.2 Conductance measurements

Measurements are controlled by a LabVIEW program. The program initially sweeps the piezo voltage from 0 up to 250 V while applying a bias voltage and records the current. Data recorded for increasing piezo voltage is called the breaking trace, whereas the data that corresponds to sweeping the piezo voltage back to 0 is called the forming trace. During the breaking trace the piezoactuator bends the substrate along with the wire to the breaking point by sweeping the voltage from 0 V to 250 V, which is indicated as a drop in the conductance to 0. After reaching the maximum piezo voltage of 250 V the program sweeps the voltage back to 0 V, thus regaining the initial position of the element. This restores the initial value of the conductance.

Breaking of the sample consists of two stages: coarse and fine. In the coarse approach, a long screw that has the piezo element attached to it is rotated until the conductance starts dropping. This means that the piezo element has bent the substrate enough, so that the wire starts breaking at the notch. The fine approach is subsequently done with the LabVIEW program, which continuously sweeps the piezo voltage. This uses the piezovoltaic properties of the element that make it elongate when a voltage is applied. Thus, by ramping up the piezo voltage step by step the element becomes longer, gradually breaking the junction.

Piezo voltage and conductance are plotted against each other to graphically illustrate the breaking process (see Figure 3.4). Meanwhile, all conductance values are collected in a histogram, which is a useful tool to show the prevailing values.

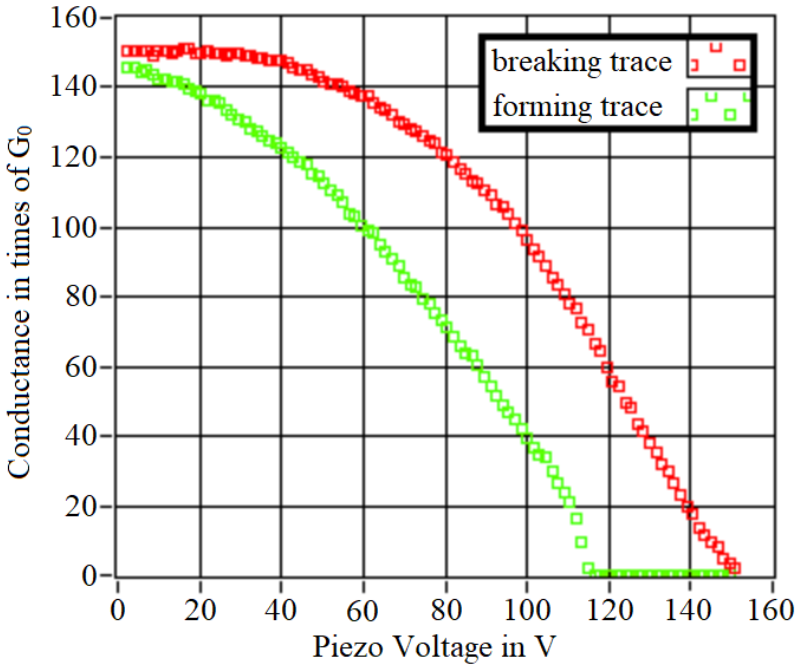

Figure 3.4: *Piezo voltage plotted against the conductance of a gold contact sample. Breaking trace data points are coloured red and labeled break, whereas forming trace data points are green and labeled form. This cycle breaks the sample and restores it to its initial value.*

In order to obtain a histogram that is statistically relevant many conductance traces, or *runs*, need to be collected. The number of runs to

complete (usually 1000) is programmed before starting the measurement. The program then continuously breaks and forms the sample the desired number of times. Due to large thermal drift while measuring at room temperature the break junction drifts out of contact beyond the range of the piezo element; the contact is broken without the piezo being able to form it again. A feedback function is implemented into the LabVIEW program to compensate for thermal drift. During the breaking trace, whenever the conductance value goes below a predefined threshold value (usually $10^{-5}G_0$) for more than 15 consecutive data points, indicating a broken junction, the piezo voltage will not sweep through to 250 V, but will rather sweep back to 0 V from its current voltage. This way the sample is not bent further by the still elongating piezo element while also being susceptible for a longer time to drifting out of contact. Instead, after the contact is certainly broken the forming trace starts almost instantly. In a similar fashion, during the forming trace, whenever the conductance value exceeds a predefined threshold value (usually 10 G_0) for more than 15 consecutive data points, indicating a formed junction, the piezo voltage will not sweep back to 0 V, but will rather sweep towards 250 V again. Hence, the effects of thermal drift on the junction are compensated, keeping it within the piezo element's range.

The LabVIEW program used for previous electrical measurements was not sufficiently fast to collect large data sets. In order to improve the speed of the program, its data flow structure had to be modified. In the previous version for every cycle of breaking and forming the incoming data points (i.e. the current) would be individually acquired by the DAQ within a while-loop structure. It would start the acquisition task, collect one value for the current and then stop the task and thus complete one loop. This process would be repeated 200 times to collect 200 values for the current. When the task is stopped after one iteration of the loop it will return to a previous task, so that the acquisition task needs to be started again in a next iteration. On average one break-form cycle took 6 seconds to complete. We implemented a solution to speed up the data collection with an advanced DAQ control function. This gave the opportunity to explicitly start the acquisition task before the loop structure and stop it after the loop completes. In the time between starting and stopping the task the loop iterates 200 times while this particular task is in the running state. Hence, it does not have to start or stop the acquisition task at every iteration, which reduces the execution time [20]. As a result, one break-form cycle requires 0.8 seconds to collect 200 data points, allowing for measurements that are more than seven times faster than before.

3.3 Sample preparation

As a substrate we used a phosphorous bronze wafer with dimensions of approximately 22 x 4 x 1 mm. The top side is covered with kapton tape in order to electrically insulate the sample wire from the substrate. The gold wire used in the experiment has 99.99% purity and has a diameter of 0.2 mm. The wire is cut a few millimeters shorter than the substrate length. We cut the wire by placing it on a rough surface and then sliding it under a razor blade mounted on a depth micrometer. This makes a cilindrical notch in the middle of the wire. Afterwards, the two ends of the notched wire are glued to the substrate with nail polish to keep the wire in place (see Figure 3.1).

The next step is to make sure that the notch can be broken in a controlled way. In order to assure that the wire will not move while the substrate is bending, an epoxy glue, Stycast, is deposited on both sides of the notch. Stycast is cured at 100°C in an oven for several minutes.

The last step of sample preparation is the attachment of electrodes. Copper wires are connected to the gold wire with conducting silver epoxy on both sides of the notch. The sample is then placed in the sample holder and mounted on the dipstick, as in Figure 3.5b.

3.4 Molecule preparation and deposition

We used the oligophenylene ethynylene (OPE3) molecule in all measurements performed in this thesis (see Figure 3.6). It consists of three benzene rings with acetyl groups attached to sulfur anchoring groups at both ends. The acetyl groups protect the molecule from forming polymers. Before deposition the molecules need to be deprotected so they can bind to the gold electrodes in the junction.

First, the OPE3 powder is dissolved using dichloromethane (DCM) solvent. To prepare a solution with an OPE3 concentration of 1 mmol $\cdot$ L^{-1}, 1 mg of OPE3 is dissolved in 2.3 mL DCM. As deprotective agent a tetrabutylammonium hydroxide (TBAH) is used. Every TBAH molecule can

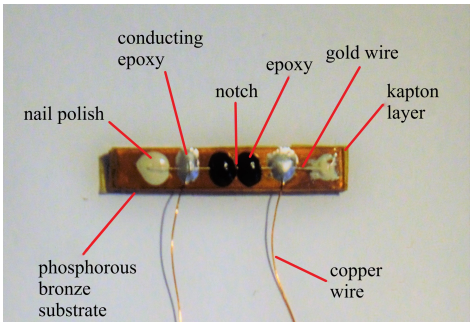

Figure 3.5(a): *A fully prepared sample. The notch is in the middle of the gold wire between the two black epoxy blobs.*

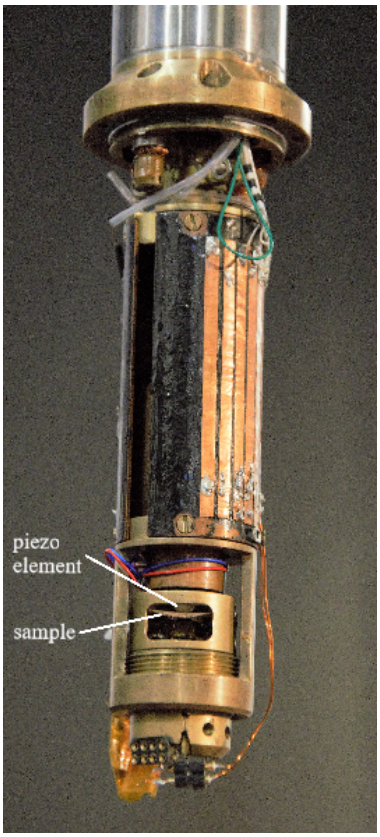

Figure 3.5(b): *The sample placed in the sample holder. Electrodes are connected to the dipstick's internal wiring. The piezo element is located in the middle of the bottom side of the sample.*

remove one protecting acetyl group of the OPE3, therefore the concentration of the TBAH solution has to be 2 mmol $\cdot$ L^{-1} or higher. We have chosen a concentration of 100 mmol $\cdot$ L^{-1} to ensure that all OPE3 molecules are deprotected. The TBAH molecules are also dissolved with DCM; 1.5 g of TBAH is dissolved in 19.3 mL DCM.

Subsequently, both solutions are sonicated for 30 minutes to fully dissolve the compounds. Deprotection is done by adding 42 μL of TBAH solution to 2 mL of OPE3 solution. The colour of the mixed solution should change from white to a dim yellow. It is necessary to deposit a droplet of the solution on the junction right after deprotection before the chemical reaction starts reverting.

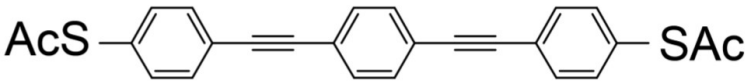

Figure 3.6: *The OPE3 molecule structural formula. Both ends have a protecting acetyl group labeled Ac and a sulfur atom labeled S that binds to the gold electrodes.*

For every molecule deposition a new sample is used. Before each deposition the gold wire is broken and reformed 500 times to test the notched wire. The droplet of 5 μL is deposited with a pipette on top of the junction, while the contact is formed. The droplet evaporates rather quickly, within 10 to 20 seconds. The dipstick is then closed and evacuated by the turbo pump. Once the desired low pressure is reached, we start the LabVIEW program and obtain conductance traces.

Chapter 4

Results and discussion

First, the experimental results of a gold-gold break junction are interpreted and compared to previous measurements. These results serve both as a test of the set-up and the LabVIEW program as well as a reference for the gold-molecule-gold junction. Second, the data of the OPE3 experiment are analysed and discussed.

4.1 Gold break junction conductance

A typical conductance break and form trace for gold junctions was already shown in Figure 3.4. That particular junction had a relatively large contact, which is displayed by the high value for the conductance ($\sim 150G_0$) when the contact is formed. Figure 4.1 shows a break-form trace for a gold junction with a smaller contact ($\sim 16G_0$). Increasing the piezo voltage decreases the conductance in steps. The short horizontal chains of data points are called *plateaus*. These occur at favorable configurations of conductance channels, usually at integer values of 1 G_0. Most notably, there is a long plateau at 1 G_0, indicating a conductance channel consisting of a single atom or even a chain of single atoms. This plateau is also the last stable configuration before the wire breaks and the conductance drops to 0.

Figure 4.1 also shows that the broken wire does not reform instantly (green data points). It takes some time before there is a nonzero conductance value again. When the single-atom chain breaks the tension of the chain is relieved and the atoms reconfigure to the loose ends of the wire.

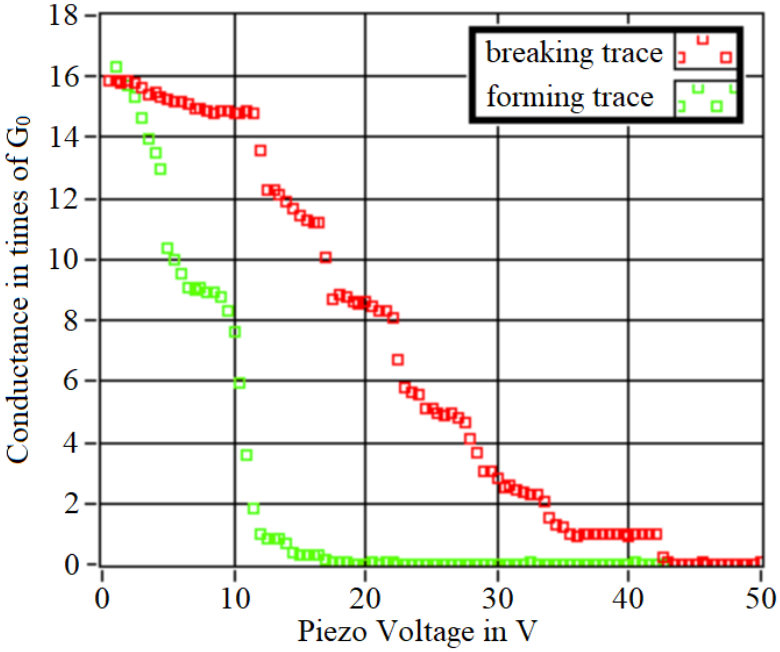

Figure 4.1: *Conductance trace of a gold-gold junction (V_B = 80 mV). Red data points indicate the conductance value for increasing piezo voltage (breaking trace), whereas the green points show the conductance for decreasing piezo voltage (forming trace). The trace shows horizontal plateaus, indicating a favorable conductance channel at that conductance value.*

Therefore, while forming the wire again, it takes a slightly larger displacement for these ends to make contact and establish a conductance. That is one of the reasons for the hysteresis in the break-form cycle. Another reason is thermal drift that occurs at room temperature. This can drift the ends of a broken contact further away, so that the formation of the contact takes a longer time. As discussed in section 3.2, a feedback function was implemented to compensate for thermal drift.

Not every plateau is exactly at an integer value of G_0. For instance, the conductance value of the plateau between 2 G_0 and 3 G_0 is non-integer. When there is an equal number of atoms on either side of the junction in contact with each other, where an atom on the left side of the junction contacts just one atom on the right side of the junction, the conductance values are expected to be around integer values of G_0. Namely, every atomic contact constitutes one conduction channel with a conductance value of 1 G_0. For any other configuration where there is not an equal number of atoms

on both sides of the junction or where an atom on the left contacts more than one atom on the right there will be conductance values that are in between integer values of G_0. That is, in this case there is a different number of conduction channels due to the atomic configuration, leading to non-integer conductance values.

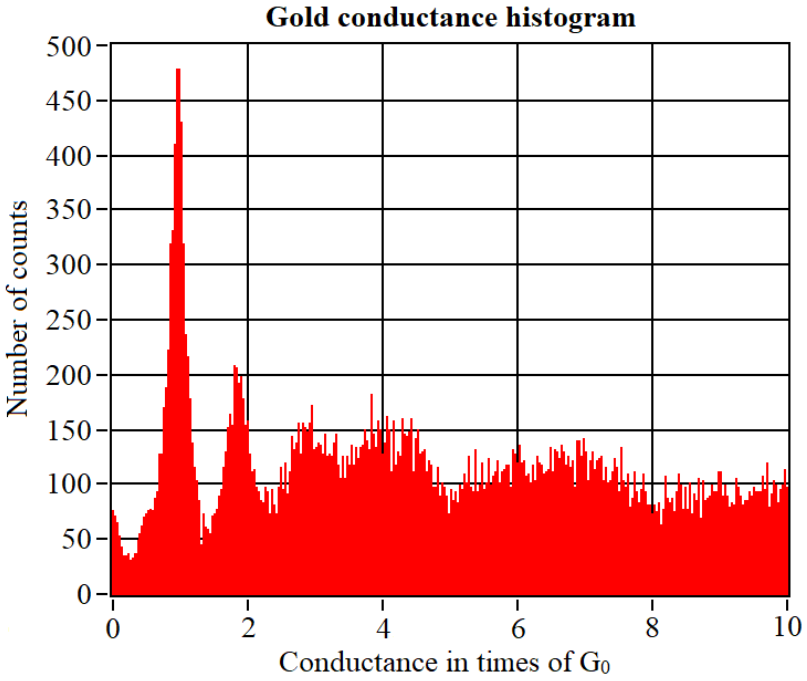

Figure 4.2: *A histogram of conductance for a gold-gold junction, containing conductance values of 1000 break-form cycles, recorded in 11 minutes. The measurement is performed at room temperature in vacuum. A large peak is visible around a value of one conductance quantum (1 G_0).*

In Figure 4.2 a histogram of a gold-gold junction is shown. This histogram displays conductance values between 0 and 10 G_0. A conductance of exactly zero is left out on purpose, because this value is measured every cycle when the wire breaks and it does not give any relevant information about the breaking process. Conductance values higher than 10 G_0 are also not included in the histogram.

The histogram shows peaks around values of 1, 2 and 3 G_0. As discussed before, the conductance of an atomic-sized junction tends to be around integer values of the quantum of conductance, especially around the relatively stable 1 G_0. In this figure the peak around 1 G_0 is also the

highest. After 3 G_0 the histogram flattens out and shows a relatively constant number of counts for all conductance values. Around those values the number of conductance channels is large and, as a result, there is no clear preference for any value in particular.

4.2 OPE3 conductance

After preparing and depositing the OPE3 as described in the previous chapter and evacuating the dipstick to a pressure of $1 \cdot 10^{-4}$ mbar we started the measurement. Conductance data of 1650 break-form cycles were obtained. The corresponding histogram can be seen in Figure 4.3.

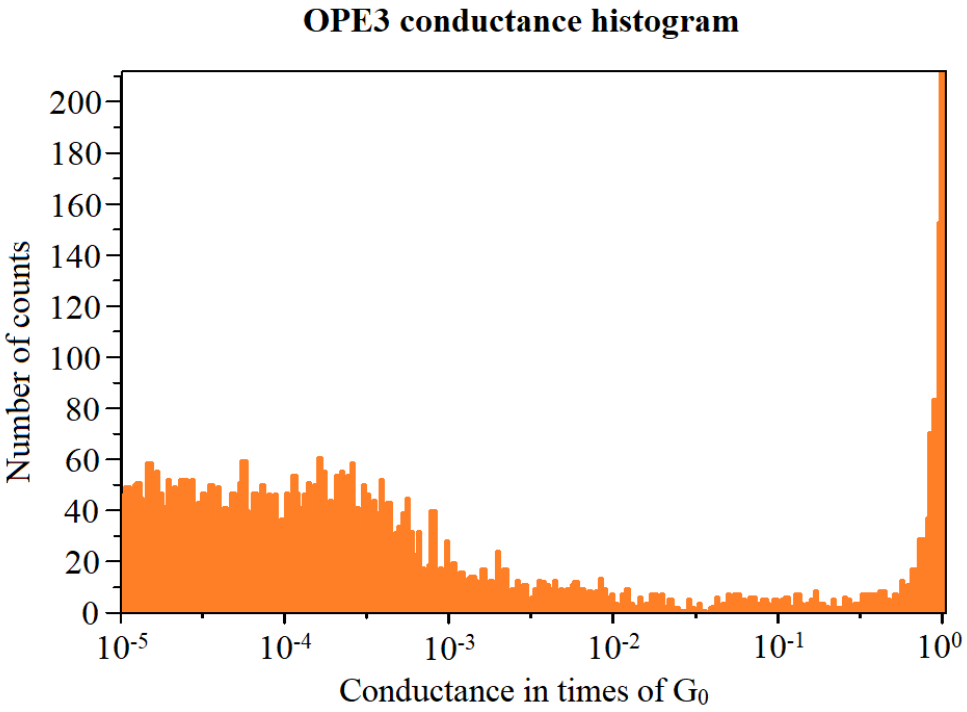

Figure 4.3: *Histogram of the conductance values of a gold-OPE3-gold junction from 1650 break-form cycles, recorded in 18 minutes. Conductance is plotted on a logarithmic scale. A peak is observed around* $5 \cdot 10^{-4} G_0$*, indicating the presence of molecules.*

To be able to show a large range of conductance values below one quantum of conductance, where the conductance of OPE3 is expected to

Version of June 14, 2018– Created June 14, 2018 - 11:25

be found, a logarithmic scale is used for the horizontal axis. Values below $10^{-5}G_0$ are excluded, because these are close to the lowest measurable conductance values of the amplifier. The conductance values of the histogram thus range from $10^{-5}G_0$ to 1 G_0. The histogram is constructed by taking the log_{10} of every measured conductance value and sorting the resulting values in size. This leads to values between -5, corresponding to a conductance of $10^{-5}G_0$, and 0, which corresponds to 1 G_0. These values are collected in 250 equally spaced bins between -5 and 0, so with every bin having a width of 0.02.

Similar to the gold histogram there is a peak around 1 G_0, on the far right side of the figure. This peak represents the instances during breaking and forming of the wire with no molecules in the junction. On the left side of this peak there is a small number of conductance values until $10^{-3}G_0$. This is in accordance with the histogram of a gold junction (see figure 4.4), where there is a flat tail from the peak of 1 G_0. After that, however, a new peak starts to emerge around $5 \cdot 10^{-4}G_0$, showing the presence of the OPE3 molecule in the junction. The peak is very broad though and not necessarily obvious from this graph.

One explanation for the broad peak is the inevitable presence of adsorbents on the sample. In principle every new sample is broken in vacuum in an attempt to minimise the amount of adsorbents on the electrode surfaces in the junction, but when the molecules are deposited the vacuum has to be broken and the sample is exposed to air. The effects of adsorbents on the sample are small, but can nevertheless influence the measurements. Another explanation is the influence of the temperature on the measurements. Measuring at room temperature does not entail the advantages of measuring at cryogenic temperatures. Most importantly, the contact between the molecule and the leads stabilises at low temperatures, so that favorable configurations of the atoms in the junction are measured more frequently, leading to sharper peaks in the histogram. At room temperature this does not occur, so peaks in those histograms are generally broader.

In an attempt to make the molecule data more insightful and more meaningful the data from a gold histogram with the same range of lower conductance values is subtracted from the OPE3 histogram. From the lower conductance histograms of gold and OPE3 it appears that there is a similar number of counts in the region between 10^{-5} and $10^{-4}G_0$, which implies that this is not caused by the presence of molecules. While both

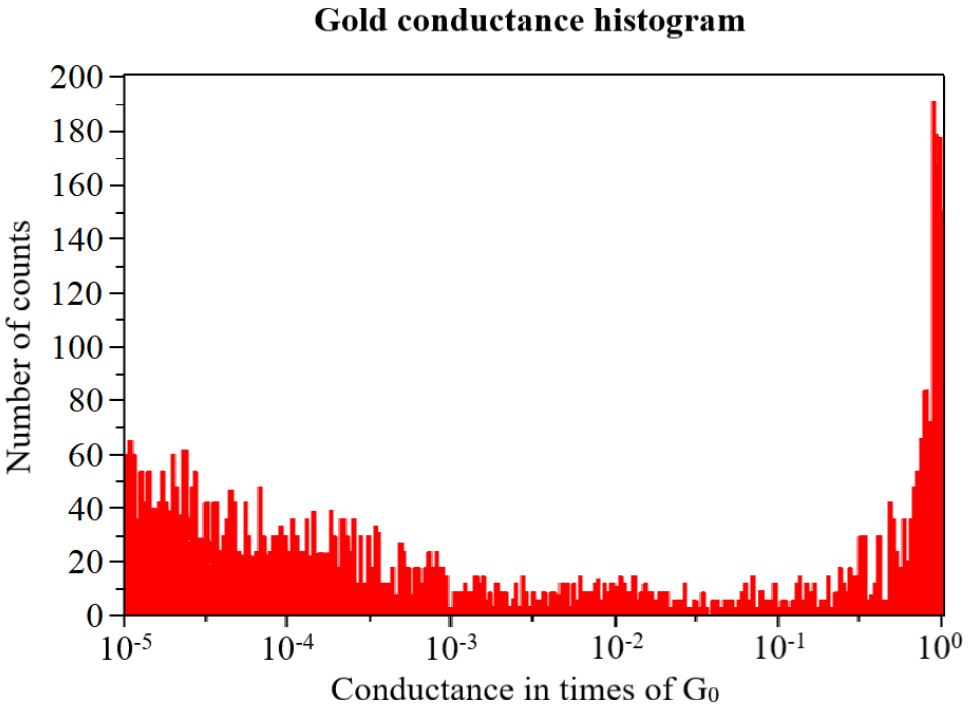

Figure 4.4: *Histogram of the low conductance values of a gold-gold junction from 1400 break-form cycles, recorded in 13 minutes. Conductance is plotted on a logarithmic scale.*

histograms also have a similar number of counts between 10^{-3} and $10^{-1}G_0$ this is expected, whereas said region is somewhat anomalous. By subtracting the gold histogram from the OPE3 histogram these values are eliminated and only pure OPE3 data is expected to remain.

Hence, the histogram in Figure 4.4 is obtained under similar conditions as the OPE3 histogram. That is, the same sample at room temperature with the dipstick evacuated to a pressure of $10^{-4}G_0$ with the same bias voltage. On the other hand the data were collected on different days, which make it susceptible to slight deviations in the immediate environment. Also, the number of completed runs is close, but not equal (gold 1400 runs, OPE3 1650 runs). Therefore the histograms are normalised before they are subtracted from each other. For each histogram the number of counts in every bin is divided by the total number of counts in that histogram, yielding the *normalised counts*. The difference between the normalised counts of both histograms is set on the vertical axis of Figure 4.5. Any negative outcome of these two has been discarded, because it is not possible that

the gold contact has more counts in the lower conductance regime than the OPE3 contact. The fact that there were negative outcomes does mean, however, that the positive values in the histogram are not completely reliable. Approximately 20% of the outcomes were negative, of which the vast majority was situated between 10^{-3} and $10^{-1}G_0$. On average these negative values had a normalised count difference of -0.001, which means that the gold contact has substantially more counts in this part than the OPE3 contact. So apparently the gold contact background is higher than that of OPE3. However, by solely discarding negative outcomes we do not take away the effect this has on the positive outcomes. These are still lowered by the relatively high values of the gold background, but the result is positive due to the presence of the OPE3. Therefore, in general, the (positive) values in the subtracted histogram are expected to be slightly higher than shown in Figure 4.5.

The histogram now has a visible peak compared to the OPE3 histogram in Figure 4.3. After fitting a Gaussian function to the histogram, we obtain a value for the peak $(1.6 \pm 0.3) \cdot 10^{-4}G_0$. The typical conductance value for the OPE3 molecule that is reported in literature [21], obtained through measurements with a lithographic MCBJ at a temperature of 4 K, is $1.2 \cdot 10^{-4}G_0$. Considering the fact that our traces were taken at room temperature the two experiments are in good agreement.

Version of June 14, 2018– Created June 14, 2018 - 11:25

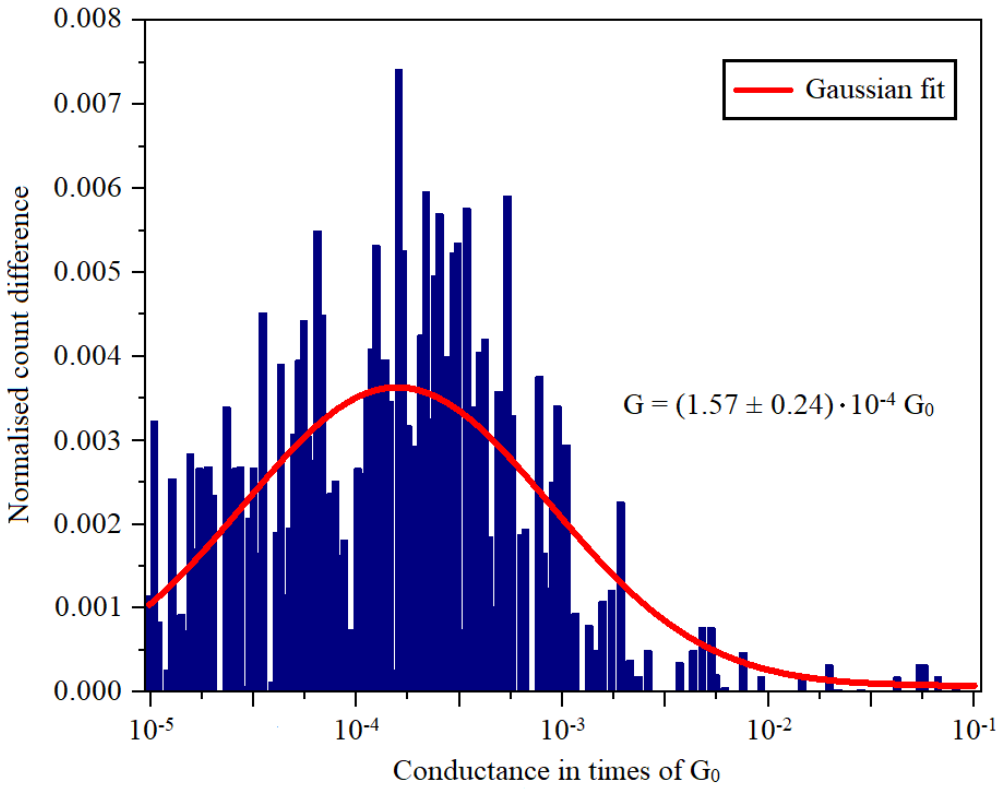

Figure 4.5: *Histogram of the difference between the conductance values of the OPE3 histogram and the gold histogram. The counts of both histograms have been normalised and subsequently subtracted from each other. Red curve represents a Gaussian fit to the histogram.*

Chapter 5

Conclusions

The first part of this research project consisted of improving an existing LabVIEW program that controls the MCBJ measurement. With a small alteration the program now runs more than 7 times faster than the previous version. One break-form cycle currently takes an average 0.8 seconds to complete.

Afterwards, the program and the entire set-up were tested at room temperature by obtaining many conductance traces of a gold junction and a conductance histogram. This was a reproduction of previous experiments and gave a result comparable to those experiments. Unfortunately, a sufficiently good vacuum could not be achieved, so the OPE3 measurements had to be taken at room temperature.

Molecule preparation methodology was slightly adapted compared to the previous method, leading to a preparation time that is thirty minutes shorter. After deposition and measurement the histogram subtracted with gold data returned a relatively accurate fitted value for the conductance peak of the OPE3: $(1.6 \pm 0.3) \cdot 10^{-4} G_0$, which is in good agreement with the value reported in literature [21] ($1.2 \cdot 10^{-4} G_0$).

5.1 Outlook

All measurements described in the results chapter were performed at room temperature. As mentioned before this comes with undesired thermal drift, which slightly distorts the measurements. Ideally, the same mea-

surements would also be done at cryogenic temperatures. The dipstick is designed to be used in a dewar of liquid helium (T $\approx$ 4 K) or liquid nitrogen (T $\approx$ 77 K) which stabilises the contact between the leads and thus reduces the thermal noise in the junction. To prevent the piezo element from sparking the pressure in the dipstick needs to be below $1 \cdot 10^{-3}$ mbar. Unfortunately, the setup used for pumping down the dipstick, consisting of a turbo pump, a vacuum connecting tube, a valve and the dipstick, had a leak at 77 K. Hence, a sufficiently low pressure could not be reached to start cooling down the dipstick. Finding a way to solve this problem, so that the dipstick can be cooled down to cryogenic temperatures, would be an obvious improvement for the experiment.

Every conductance value in this experiment is obtained by repeatedly sweeping the piezo voltage with a fixed bias voltage over the junction and measuring the current. It is also possible to conduct measurements based on I-V characteristics where the bias voltage is varied [22]. This method sweeps the bias voltage while the piezo element is slowly elongating and records the corresponding current. Even if this method is actually slower than the piezo voltage sweep, it does provide another way of obtaining a measure of the average conductance of a junction.

If this method is to be implemented it is useful to calibrate the piezo element, so that it is exactly known how increasing the piezo voltage affects the displacement of the piezo element. Even if this method is not implemented it is suggested to calibrate the piezo element before any further experiments are conducted, because it is common in this field to plot the conductance to the displacement of the piezo element instead of the piezo voltage (as has been done in this thesis). When the attenuation ratio of the sample, which is the ratio between the vertical displacement of the piezo element and the resulting horizontal displacement of the metal electrodes, is determined it is then possible to translate the piezo displacement to the electrode separation of the sample.

For future experiments it can be instructive to measure different molecules that have a similar structure. The ideal molecules are the ones that have a conjugated backbone with anchor groups on both sides, therefore immobile in a junction [21]. Oligo(phenylene vinylene) (OPV) [21] and OPE3-AC [22] are suitable replacements for the OPE3 used in this experiment.

On another note, although the measurement speed of the LabVIEW program is faster, there is still room for improvement. As it stands the

program still contains multiple functions that are unused during a conductance measurement. Removing these unnecessary parts should again increase measurement speed. The programming structure is very complex and unclear, however, making it very hard to select parts that can be removed without disturbing the critical functions of the program. It is wise to start a new research by taking care of this before the experiments are started. This will also make it easier to adapt or improve parts of the program in the process, which has proven to be necessary every now and then.

Bibliography

[1] Derek Cheung and Eric Brach. *Conquering the Electron*. Rowman & Littlefield Publishers, 2014.

[2] Samsung. Qualcomm and samsung collaborate on 10nm process technology for the latest snapdragon 835 mobile processor. `https://news.samsung.com/global/qualcomm-and-samsung-collaborate-on-10nm-process-technology\-for-the-latest-snapdragon-835-mobile-processor`, 2016. Online; accessed 22-08-2017.

[3] Konstantin Likharev. Electronics below 10 nm. *Nano and Giga Challenges in Microelectronics*, pages 27–68, 2003.

[4] J. Modod and F. Jacob. General conclusions: teleonomic mechanisms in cellular metabolism, growth and differentiation. *Cold Spring Harbor Symp. on Quant. Biol.*, 26:389–401, 1961.

[5] Timothy S. Gardner, Charles R. Cantor, and James J. Collins. Construction of a genetic toggle switch in *Escherichia coli*. *Nature*, 403:339–342, 2000.

[6] Juan Carlos Cuevas and Elke Scheer. *Molecular Electronics: An Introduction To Theory And Experiment*. World Scientific, 1 edition, 2010.

[7] John Moreland and J.W. Ekin. Electron tunneling experiments using nb-sn "break" junctions. *Journal of Applied Physics*, 58(10), 1985.

[8] C.J. Muller, J.M. van Ruitenbeek, and L.J. de Jongh. Experimental observation of the transition from weak link to tunnel junction. *Physica C: Superconductivity*, 191(3):485 – 504, 1992.

[9] S. A. G. Vrouwe, E. van der Giessen, S. J. van der Molen, D. Dulic, M. L. Trouwborst, and B. J. van Wees. Mechanics of lithographically defined break junctions. *Physical Review Letters B*, 71, 2005.

[10] M. A. Reed, C. Zhou, C. J. Muller, T. P. Burgin, and J. M. Tour. Conductance of a molecular junction. *Science*, 278(5336):252–254, 1997.

[11] Jim Greer, Anatoli Korkin, and Jan K Labanowski. *Nano and giga challenges in microelectronics*. Elsevier, 2003.

[12] Christian A Martin, Dapeng Ding, Herre S J Van der Zant, and Jan M Van Ruitenbeek. Lithographic mechanical break junctions for single-molecule measurements in vacuum: possibilities and limitations. *New Journal of Physics*, 10, 2008.

[13] Michael C. Petty. *Molecular Electronics From Principles to Practice*. Wiley, 2008.

[14] Yu. V. Sharvin and N.I. Bogatina. Investigation of Focusing of Electron Beams in a Metal by a Longitudinal Magnetic Field. *Soviet Physics Journal of Experimental and Theoretical Physics*, 29, 1969.

[15] Giuseppe Grosso and Giuseppe Pastori Parravicini. *Solid State Physics*. Oxford: Academic Press, 2 edition, 2013.

[16] Cancan Huang, Alexander V. Rudnev, Wenjing Hong, and Thomas Wandlowski. Break junction under electrochemical gating: testbed for single-molecule electronics. *Chemical Society Reviews*, 44:889–902, 2015.

[17] Jean-Pierre Launay and Michel Verdaguer. *Electrons in Molecules: From Basic Principles to Molecular Electronics*. Oxford University Press, 2018.

[18] Riccardo Frisenda. *OPE3: A Model System for Single-Molecule Transport*. 2015.

[19] Properties of piezo actuators: Ambient conditions. `https://www.piceramic.com/en/piezo-technology/properties-piezo-actuators/ambient-conditions/`. Accessed: 13-03-2018.

[20] Task state model. `http://zone.ni.com/reference/en-XX/help/370466AD-01/mxcncpts/taskstatemodel/`. Accessed: 05-06-2018.

[21] Roman Huber, Maria Teresa Gonzalez, Songmei Wu, Michael Langer, Sergio Grunder, Viviana Horhoiu, Marcel Mayor, Martin R. Bryce, Changsheng Wang, Rukkiat Jitchati, Christian Schönenberger, and Michel Calame. Electrical conductance of conjugated oligomers at the single molecule level. *American Chemical Society Journals*, 130:1080–1084, 2008.

[22] Riccardo Frisenda. *OPE3: a model system for single-molecule charge transport*. PhD dissertation, Technische Universiteit Delft, 2016.